Chapter 6

Magneto(di)electric coupling in MCr_2O_4 (M = Mn, Co, and Ni) spinel

6.1. Introduction

Multiferroics, materials in which ferromagnetism and ferroelectricity coexist, have attracted much attention in recent years [1–6]. If the coupling between the magnetic and ferroelectric order (magnetodielectric coupling) is strong enough, multiferroics potentially allow the manipulation of electric and magnetic moments by magnetic and electric fields, respectively. However, there are still rather few multiferroics known and the magnetodielectric coupling in many of them is weak. This is largely due to the fact that in typical ferroelectric oxides the creation of an electric dipole moment involves charge transfer between the occupied 2p orbitals of oxygen and the empty d-shell of the metal ions. The common mechanism of ferroelectricity thus excludes transition metals with partially-filled d-orbitals and hence the coexistence of magnetic moments and ferroelectric order [1]. Nevertheless, in recent years an increasing number of multiferroics have been discovered in which ferroelectricity arises from different mechanisms. For example, ferroelectricity can be directly induced by frustrated magnetic ordering in materials such as $TbMnO_3$, $TbMn_2O_5$, and $Ni_3V_2O_8$ [2, 4, 6], which naturally leads to strong magnetodielectric coupling. One feature common to many of the frustrated magnet multiferroics is the existence of a spiral or helical spin structure. Here, the direction of the spontaneous polarization is perpendicular to both the magnetic propagation vector and to the spin plane of the spiral. Although the microscopic mechanisms involved in the magnetodielectric coupling in this class of multiferroics are being widely studied both experimentally and theoretically, in many cases the mechanisms are not fully understood, especially regarding the strength of the coupling. Therefore, it is important to investigate magnetodielectric coupling in a wide range of frustrated-magnet

multiferroics. The materials MCr_2O_4 (M = Mn, Co and Ni) are ferrimagnetic spinels, in which the M^{2+} cations occupy the tetrahedral (A) sites and the Cr^{3+} cations occupy the octahedral (B) sites. In single crystal samples the onset of collinear ferrimagnetic ordering occurs at 51 K, 93 K and 74 K, respectively. A further magnetic transition occurs at $T_f \sim 18$ K, 26 K and 31 K, respectively [10,11]. In $CoCr_2O_4$ and $MnCr_2O_4$ a short-range-ordered (SRO) spiral component develops, giving a conical magnetic structure below T_s (see Figure 6.1). A "lock-in" transition occurs at 13 K for $CoCr_2O_4$ and at 14 K for $MnCr_2O_4$. The magnetic ground state of spinels with spiral or conical structures can be well described by the parameter u [9]:

$$u = \frac{4\tilde{J}_{BB}S_B}{3\tilde{J}_{AB}S_A} \tag{6.1}$$

Here, $\tilde{J}_{BB}$ and $\tilde{J}_{AB}$ are the nearest-neighbor (NN) interactions involving spins S_A and S_B on the A and B sites. In this theory the AA nearest-neighbor interaction is neglected. It is important to note that the possible values of u range from 0 to infinity, corresponding to configurations between a Neel ferrimagnetic structure and a state characterized by "magnetic geometric frustration" (MGF). Below u = 8/9 the magnetic structure is described as a Neel long-range ordered configuration [9], in the range from u = 8/9 to u = 1.298 the magnetic ground state is predicted to be a long-range ordered spiral structure, and above u = 1.298 the magnetic structure is predicted to be locally unstable with short-range spiral order [10]. For single crystal samples, the coherence length of the spiral reaches the order of 10 nm at low temperatures with a propagation vector q = (0.59, 0.59, 0) for $MnCr_2O_4$ and 3.5 nm with a propagation vector q = (0.62, 0.62, 0) for $CoCr_2O_4$. The corresponding values of u for $MnCr_2O_4$ and $CoCr_2O_4$ are 1.5 and 2.0, respectively [10]. In contrast, $NiCr_2O_4$ exhibits collinear antiferromagnetic ordering below T_s with the propagation vector q = (0 0 1) [11]. The value of u for $NiCr_2O_4$ is expected to be larger than that of $CoCr_2O_4$ due to the small total magnetic moment. The rather short correlation lengths (less than 10 nm) of these spiral structures are thought to be the result of weak geometrical frustration on the spinel B-site; the magnetic exchange interactions between the A and B sites are weaker than those among the B-sites and are insufficient to suppress the MGF [10]. Recently, Yamasaki et al. have reported the presence of ferroelectricity in $CoCr_2O_4$ single crystals [7], making it one of the few materials to exhibit the coexistence of ferromagnetic and ferroelectric states. The onset of polarization occurs at $T_s \sim 26$ K along the $[1\bar{1}0]$ direction and the polarization can be reversed by switching the direction of the applied magnetic field. It is to be noted that the polarization in this system is smaller than of the multiferroic $R\mathrm{MnO_3}$ perovskites due to the weak spin-orbit coupling strength of Cr^{3+} ($t_{2g}^3 e_g^0$) compared to Mn^{3+} ($t_{2g}^3 e_g^1$) [7]. The mechanism of the induced ferroelectricity in $CoCr_2O_4$ can be explained by the spin current model for magnetic ferroelectricity proposed by Katsura et al. [8]. These results prompted us to investigate the magnetic and dielectric properties of the series MCr_2O_4 (M = Mn, Co, and Ni) in order to explore the nature of

the magnetodielectric coupling in the spiral (conical) and canting magnetic structures in this system.

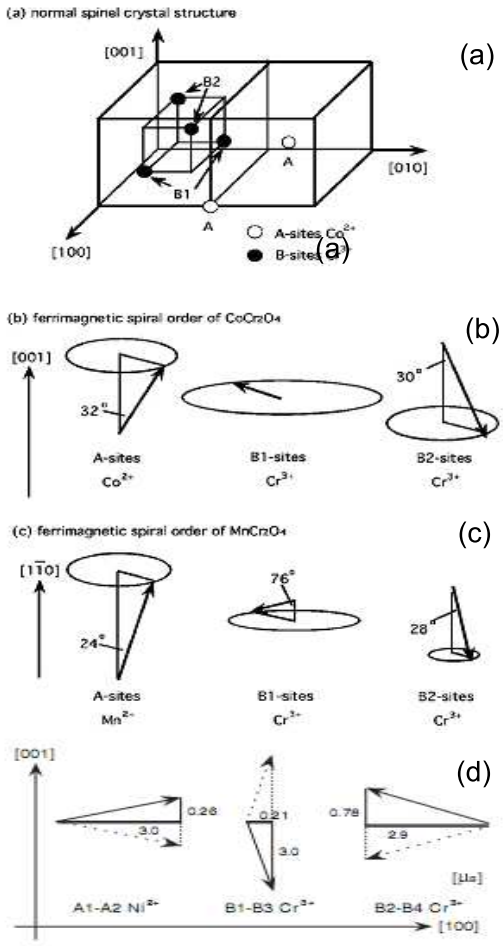

Figure 6.1: *(a) Schematic picture of sublattices in the MCr_2O_4 spinel structure: tetrahedral A-site and octahedral B1, B2 sites. The orientations of the spins on the A and B-sites are shown for (b) $CoCr_2O_4$, (c) $MnCr_2O_4$ and (d) $NiCr_2O_4$. This figure is taken from Refs. [10, 11].*

6.2. Experiment

Polycrystalline samples of MCr_2O_4 (M = Mn, Co, and Ni) were prepared by solid state reaction using a stoichiometric mixture of $MnCO_3$, CoO, NiO and Cr_2O_3. The samples were first sintered at 1000°C for 12 h and then at 1300°C for 24 h in flowing argon, with intermediate grinding. Two samples of $MnCr_2O_4$ were prepared. Sample 1 was compressed hydrostatically at 600 bar in a rubber tube into a rod of diameter 7 mm and length 50 mm (this sample was prepared for the purpose of crystal growth in a floating zone furnace) before heating at 1300°C in flowing argon. To prepare sample 2, sample 1 was crushed and pelletized at 0.27 bar, before sintering at 1300°C in flowing

argon for 24 h. We attempted to grow single crystals using the floating zone technique, but due to the evaporation of Cr^{3+} this was not successful. We also tried to grow single crystals using the flux technique, but this also failed due to leakage from the platinum crucible. X-ray powder diffraction at room temperature was performed using a Bruker D8 diffractometer with Cu-Kα radiation. Magnetization measurements were performed using a Quantum Design MPMS-7 SQUID magnetometer. The capacitance was measured using an AH-2500A capacitance bridge and a Quantum Design PPMS.

6.3. Results

6.3.1. Structural properties

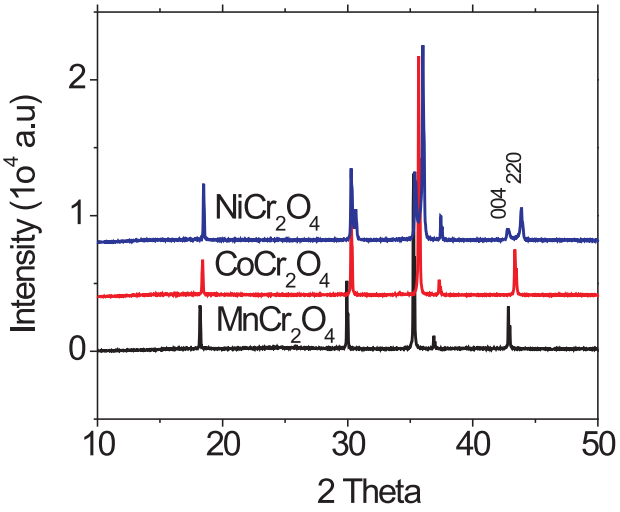

Figure 6.2: *X-ray powder diffraction patterns of MCr_2O_4 (M = Mn, Co, and Ni) at room temperature.*

Room-temperature X-ray powder diffraction measurements showed that the MCr_2O_4 (M = Mn, Co, Ni) samples were single-phase (see Figure 6.2); $MnCr_2O_4$ and $CoCr_2O_4$ adopt the cubic spinel structure with space group F$d\bar{3}m$ (227), with lattice parameters of 8.43727(6) Å and 8.33335(9) Å, respectively. In contrast, $NiCr_2O_4$ adopts a tetragonal spinel structure with space group $I4_1/amd$ (141) and lattice parameters of a = 5.83510(12) Å and c = 8.43320(14) Å. The lattice parameters of all three synthesized samples are in good agreement with those previously reported [12–14]. In spinel MCr_2O_4, M^{2+} occupies the tetrahedral site and Cr^{3+} occupies the octahedral site. In $NiCr_2O_4$ the tetrahedral site containing Ni^{2+} ($e^4t_2^4$) has a Jahn-Teller distortion and is elongated along the c-axis, giving rise to the tetragonal structure.

6.3.2. Magnetic properties

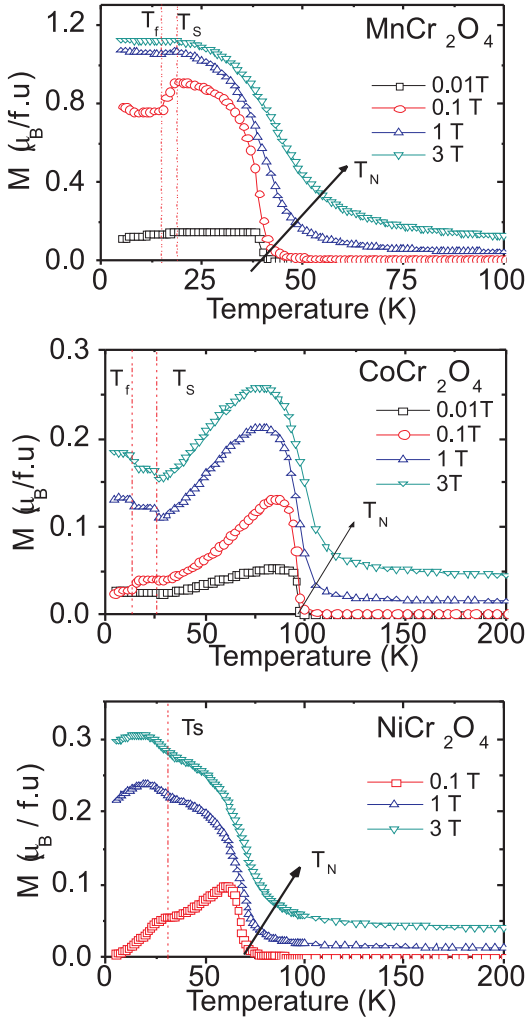

Figure 6.3: *Temperature dependence of magnetization of (a) $MnCr_2O_4$ (sample 1), (b) $CoCr_2O_4$, and (c) $NiCr_2O_4$ under different applied magnetic fields. The samples were cooled in zero field (ZFC).*

The magnetic susceptibility of MCr_2O_4 (M = Mn, Co, Ni) at different magnetic fields is shown in Figure 6.3. The onset of ferrimagnetic ordering is observed at 43 K for $MnCr_2O_4$, 97 K for $CoCr_2O_4$, and 75 K for $NiCr_2O_4$ in a field of 0.1 T. In all of the samples the value of T_c increases with applied magnetic field and the transition becomes broader. Other anomalies are observed at $T_s \sim 18$ K and $T_f \sim 15$ K for $MnCr_2O_4$, and $T_s \sim 27$ K and $T_f \sim 15$ K for $CoCr_2O_4$, which correspond to the temperatures where the spiral component appears and to the "lock-in" transition at which the spiral becomes fully developed, as reported by Tomiyasu et al. [10]. In $MnCr_2O_4$, both anomalies become less well defined when the field is increased. In $CoCr_2O_4$, the anomalies are still visible up to at

least 3 T. For $NiCr_2O_4$ only one anomaly is observed at $T_s \sim 31$ K, which corresponds to the onset of the canted antiferromagnetic structure [11]. Similar to $CoCr_2O_4$, this anomaly is not affected by increasing the magnetic field up to 3 T. Figure 6.4 shows plots of magnetization versus field at various temperatures. The spontaneous magnetizations of $MnCr_2O_4$, $CoCr_2O_4$ and $NiCr_2O_4$ at 5 K are estimated to be approximately 1 μ_B/f.u., 0.15 μ_B/f.u. and 0.2 μ_B/f.u., respectively, by linearly extrapolating the high-field magnetization to zero field. All of these values are in good agreement with those previously reported [10–12, 16]. These results indicate that as the magnetic moment on the A-sites decreases, the exchange interaction between the A and B-sites leads to an increase of the cone angle associated with the A, B1, and B2 sites. According to the theory of Lyons et al. [9], this is also associated with an increase in the value of u. Larger values of u will result in a greater degree of hysteresis in the magnetization versus field loops.

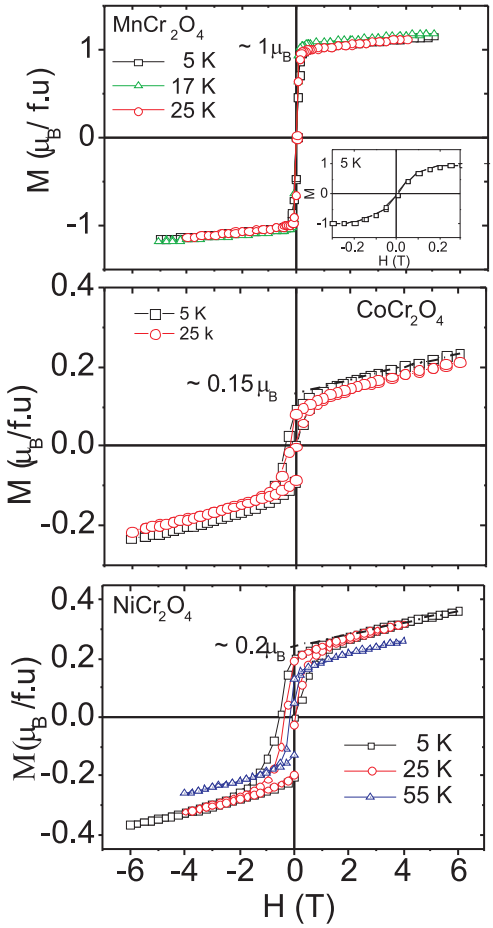

Figure 6.4: *Field dependence of magnetization at various temperatures for (a) $MnCr_2O_4$ (sample 1), (b) $CoCr_2O_4$, and (c) $NiCr_2O_4$.*

6.3.3. Dielectric properties

The temperature dependence of the dielectric constant of MCr_2O_4 (M = Mn, Co, Ni) is shown in Figure 6.5. Three anomalies are apparent for $MnCr_2O_4$ and $CoCr_2O_4$, at approximately the same temperatures as the magnetic transitions. The small differences in transition temperatures are probably due to differences in temperature between the sensor and sample during heating. For $MnCr_2O_4$ the temperature dependence of the dielectric constant was measured for both samples. In sample 1 (pelletized at 600 bar), the dielectric constant increases with decreasing temperature and reaches a plateau at 43 K, corresponding to the ferromagnetic transition. The dielectric constant then falls more rapidly at T_s and shows a further anomaly at T_f, which is suppressed with increasing magnetic field. For sample 2, the dielectric constant decreases with decreasing temperature and changes slope at T_s. Although the behavior at T_s and T_f is similar to that of sample 1, no anomaly is seen at the magnetic ordering temperature and the reason for the difference in slope above T_N is unclear. We suggest that this phenomenon may be due to the difference in density of the two polycrystalline samples. In this case, extrinsic effects due to factors such as the electrodes and contacts, grain boundaries and porosity would play a significant role.

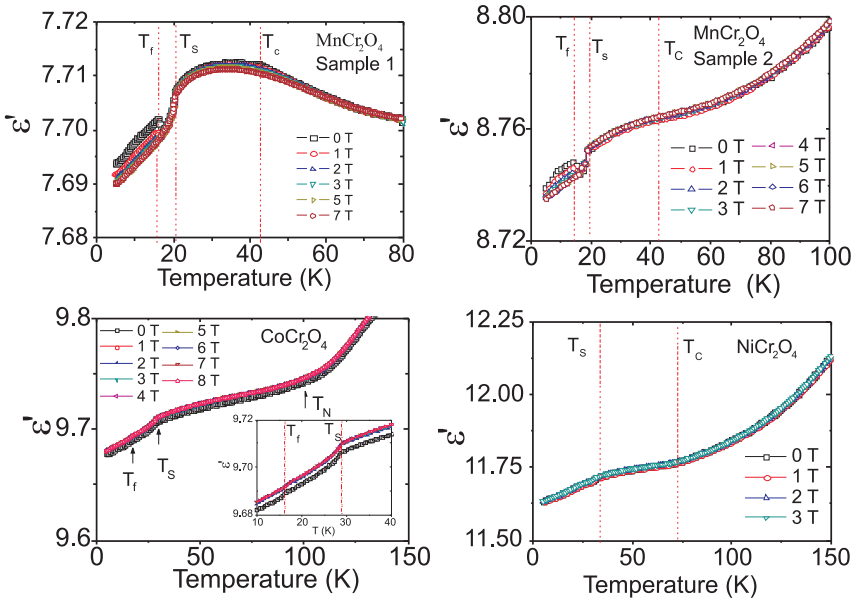

Figure 6.5: *Temperature dependence of dielectric constant at various magnetic fields for (a) $MnCr_2O_4$ (sample 1), (b) $MnCr_2O_4$ (sample 2), (c) $CoCr_2O_4$, and (d) $NiCr_2O_4$.*

The dielectric constant of $CoCr_2O_4$ has previously been measured by Lawes et al. [13]; anomalies were observed at $T \sim 50$ K and $T_s \sim 27$ K and were assigned to the onset of short-range magnetic

order and long-range magnetic order, respectively. It was argued using specific heat data that the correlation length of the spiral state is different in single crystal and polycrystalline samples; in the latter a long-range ordered (LRO) spiral develops below T_s. In contrast, we only observe anomalies at 27 K and 15 K (see Figure 6.5(b)); these agree with the onset temperature of the SRO conical structure and the "lock-in" transition reported by Tomiyasu et al., who carried out magnetic measurements and neutron diffraction measurements on single crystal samples [10]. The dielectric anomaly at T_f becomes less well-defined with increasing magnetic field. In $NiCr_2O_4$, the temperature dependence of the dielectric constant shows changes in slope at T_N and T_s; the profile remains unchanged on applying magnetic fields of up to 3 T.

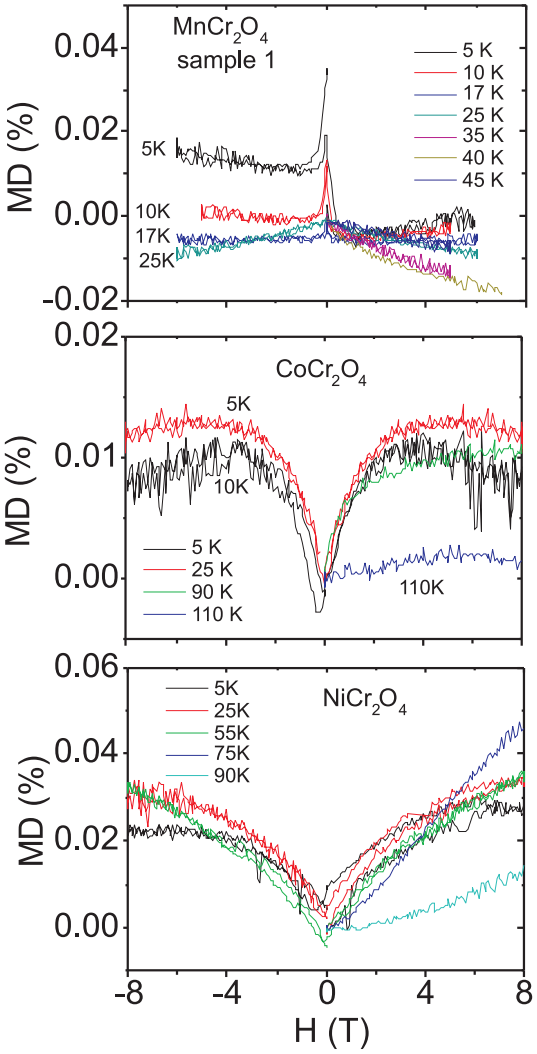

Figure 6.6: *Dielectric constant as a function of magnetic field (in the form of magnetodielectric response- see text for definition) for (a) $MnCr_2O_4$, (b) $CoCr_2O_4$, and (c) $NiCr_2O_4$.*

Figure 6.6 shows the magnetocapacitance of the three compounds, that is, the dielectric constant as a function of magnetic field. We define the magnetodielectric response (MD) as MD = (ε(H)-ε(0))/ε(0), where ε(H) is the dielectric constant under field and ε(0) is the dielectric constant in the absence of any magnetic field. For $MnCr_2O_4$, the dielectric constant suddenly drops (negative magnetocapacitance) in very low magnetic fields. Moreover, the unusual magnetocapacitance profile develops an asymmetric shape below T_f; it is symmetric at temperatures above T_s. In contrast, the magnetodielectric profiles of $CoCr_2O_4$ and $NiCr_2O_4$ indicate a sharp increase in the dielectric constant in low magnetic fields, and are symmetric at all temperatures. The magnitude of the magnetodielectric response increases in the order $MnCr_2O_4$, $CoCr_2O_4$ and $NiCr_2O_4$.

6.4. Discussion

In order to investigate the magnetodielectric coupling in spinel MCr_2O_4 (M = Mn, Co, Ni), we consider the trend of the dielectric constant below T_s. Because MCr_2O_4 is non-polar between T_c and T_s [7], we have taken a linear extrapolation of the dielectric constant from this region down to low temperature. The insets in Figure 6.7 show the residual dielectric constant after subtraction of the linearly extrapolated values and division by the dielectric constant at 5K (-$\triangle\varepsilon/\varepsilon_{5K}$). The residual dielectric constant, that is, the deviation from the extrapolated value, increases in the order $MnCr_2O_4$, $CoCr_2O_4$ and $NiCr_2O_4$. The magnitude of the residual dielectric constant corresponds to the magnetodielectric coupling strength, thus large deviation from the linearly extrapolated values indicates large magnetodielectric coupling. In order to explain this phenomenon, we consider the spin-orbit coupling and orbital degrees of freedom of M^{2+}. The spin-orbit coupling is defined as λL.S where L is the orbital angular momentum and S is the total spin. In $MnCr_2O_4$, Mn^{2+} (d^5) has L=0 hence no spin-orbit coupling. For $CoCr_2O_4$, Co^{2+} (d^7) has , in tetrahedral coordination, a non-quenched orbital orbital moment and spin orbit coupling can affect the magnetodielectric coupling. For $NiCr_2O_4$, The Ni^{2+} (d^8) in tetrahedral coordination is Jahn-Teller active. For this system we observe the largest magnetodielectric coupling. We conclude that the orbital degree of freedom for Ni^{2+} provides stronger coupling than the spin-orbit coupling in $CoCr_2O_4$. A similar observation was previously made in MnT_2O_4 (T = Mn, V, Cr) [17], where it was proposed that the presence of orbital degrees of freedom is a key factor in the correlation between magnetic properties, dielectric properties and the crystal structure.

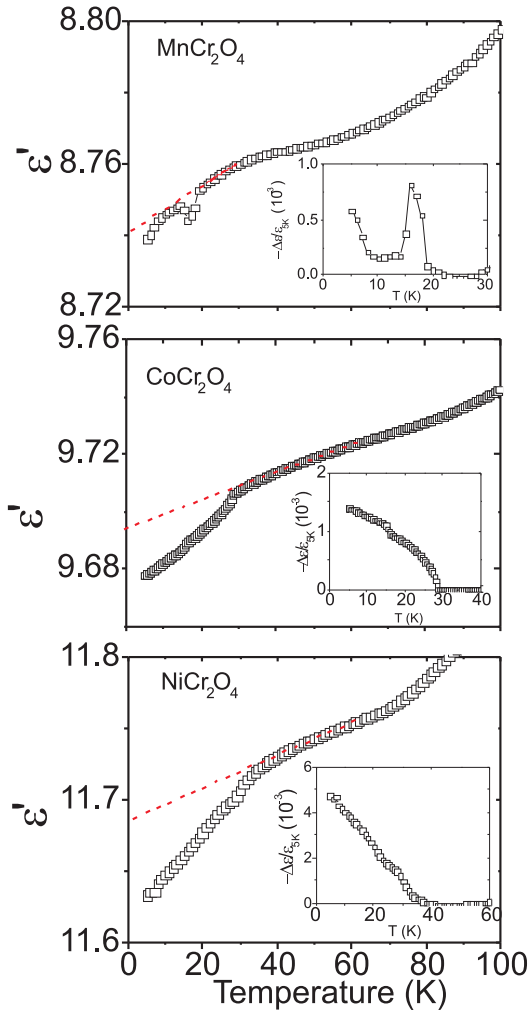

Figure 6.7: *Temperature dependence of dielectric constant of MCr_2O_4 (M = Mn, Co, Ni). The insets show the negative of the residual dielectric constant after subtraction of the linearly extrapolated value and division by the dielectric constant at 5K (-$\triangle\varepsilon/\varepsilon_{5K}$).*

The LRO ferrimagnetic structure and the SRO spiral structure are known to coexist below T_f in $MnCr_2O_4$ and $CoCr_2O_4$. In $MnCr_2O_4$, there are two sets of spiral domains with propagation vectors parallel to the [110] and -[110] directions for an easy axis parallel to $[1\bar{1}0]$. In contrast, $CoCr_2O_4$ has four spiral domains with propagation vectors $\pm$[110] and $\pm[1\bar{1}0]$ for an easy axis along the [001] direction [10]. Moreover, the correlation length of the spiral in single crystal $MnCr_2O_4$ (9.9 nm) is larger than that in $CoCr_2O_4$ (3.1 nm). This difference might cause the dielectric anomaly at T_f to be more pronounced in $MnCr_2O_4$ than in $CoCr_2O_4$. For $MnCr_2O_4$, the dielectric anomaly at T_f is suppressed by increasing the magnetic field. We believe that this phenomenon indicates an increasing correlation length of the spiral structure. The spins will tend to align with the magnetic

field, and consequently the propagation vectors in the two domains will also become aligned in the same direction. Thus, the transition to the SRO spiral state at T_f will be suppressed, along with the dielectric anomaly here. For $CoCr_2O_4$ the anomaly at T_f is much smaller, hence it is difficult to observe any change on the application of a magnetic field. The asymmetric magnetodielectric behavior in $MnCr_2O_4$ is more difficult to explain. A similar phenomenon has previously been observed in Mn_3O_4, for which it was argued that the asymmetry is due to the magnetic hysteresis present at low temperatures [15]. We believe that this argument is invalid because we do not observe magnetic hysteresis in our magnetization measurements of $MnCr_2O_4$. Moreover, in $CoCr_2O_4$ and $NiCr_2O_4$ where magnetic hysteresis is observed, the magnetodielectric behavior is symmetric. We suggest that the increasing correlation length of the spiral structure with increasing field in $MnCr_2O_4$ might be responsible. Further investigation of the magnetodielectric response on single crystals might give a better understanding of this phenomenon.

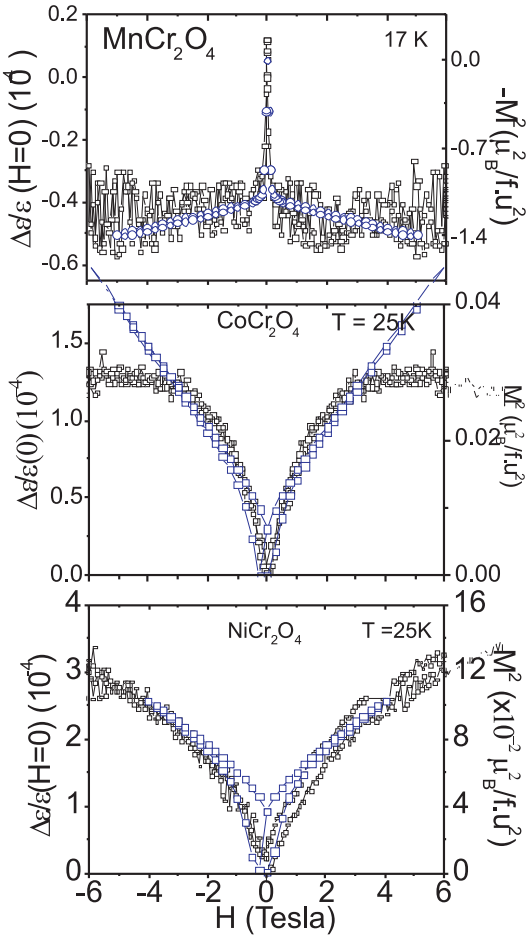

Figure 6.8: *Magnetodielectric response (black data points) and the square of the magnetization (colored data points) as a function of magnetic field for (a) $MnCr_2O_4$, (b) $CoCr_2O_4$, and (c) $NiCr_2O_4$.*

In Figure 6.8 we superimpose plots of the magnetodielectric response and the square of the magnetization for all three samples. The two types of plot overlie each other more closely for $MnCr_2O_4$ than for $CoCr_2O_4$ and $NiCr_2O_4$. Nevertheless, the magnetodielectic ($-\triangle\varepsilon/\varepsilon_{H=0}$) response scales approximately with the square of the magnetization (M^2) for all three samples. This suggests that the magnetodielectric coupling originates from the P^2M^2 term in the free energy expansion, which is always allowed by symmetry in ferroelectromagnetic materials [11]. The magnitude of the magnetodielectric response ($-\triangle\varepsilon/\varepsilon_{H=0}$)) increases in the order $MnCr_2O_4$, $CoCr_2O_4$ and $NiCr_2O_4$. This result is consistent with the residual dielectric constant ($-\triangle\varepsilon/\varepsilon_{5K}$) at low temperatures in Figure 6.7. Nevertheless, the magnetodielectric effect in these spinel materials is small compared to other multiferroics such as $TbMnO_3$, which has a magnetocapacitance of 10%, even though the ferroelectricity in $MnCr_2O_4$ and $CoCr_2O_4$ is also induced by the magnetic structure. This result indicates that improper ferroelectricity, such as ferroelectricity induced by the magnetic structure, is no guarantee of obtaining a large magnetodielectric effect.

6.5. Conclusion

We have investigated the magnetic and dielectric properties of polycrystalline samples of the spinels MCr_2O_4 (M = Mn, Co, and Ni). Coupling between the dielectric and magnetic properties is observed at the onset of the magnetic spiral structure (T_S) and at the "lock-in" transition (T_f) in $MnCr_2O_4$ and $CoCr_2O_4$, and also at the onset of the canted structure (T_s) in $NiCr_2O_4$. The strength of the magnetodielectric coupling in this system can be explained by taking into account the spin-orbit coupling and presence or absence of orbital degrees of freedom on the tetrahedral site. The dielectric anomaly at T_f for $MnCr_2O_4$ is suppressed under applied magnetic fields, indicating that the correlation length of the spiral structure increases with field. This effect might also be responsible for the asymmetric behavior of the magnetodielectric response in $MnCr_2O_4$ below T_f. The magnetodielectric response in applied magnetic fields scales with the square of the magnetization for all three samples. Thus, the magnetodielectric coupling in this state appears to originate from the P^2M^2 term in the free energy. The magnetodielectric effect in all three MCr_2O_4 materials is very small, which implies that frustrated materials showing magnetically induced ferroelectricity do not necessarily exhibit large magnetodielectric effects.

Bibliography

[1] N. Hill, J. Phys. Chem. B, **104**, 6694, (2000).

[2] T. Kimura, T. Goto, H. Shintani, K. Ishizaka, T. Arima, and Y. Tokura, Nature **429**, 55 (2003)

[3] T. Kimura, S. Kawamoto, I. Yamada, et al., Physical Review B **67**, 180401 (2003).

[4] N. Hur, S. Park, P. A. Sharma, et al., Nature **429**, 392 (2004).

[5] S.-W. Cheong and M. Mostovoy, Nat. Mater. **6**, 23(2007).

[6] G. Lawes et al. Phys. Rev . Lett. **95**, 087205 (2005)

[7] Y. Yamasaki, S. Miyasaka, Y. Kaneko, et al., Phys. Rev. Lett. **96**, 207204 (2006).

[8] H. Katsura, N. Nagaosa, and A. V. Balatsky, Phys. Rev. Lett. **95**, 057205 (2005).

[9] D. H. Lyons, K. Dwight, T. A. Kaplan, et al., Phys. Rev. **126**, 540 (1962).

[10] K. Tomiyasu, J. Fukunaga, and H. Suzuki, Phys. Rev. B **70**, 214434 (2004).

[11] K. Tomiyasu, I. Kagomiya, J. Phys. Soc. Japan **73**, 2539 (2004).

[12] J. M. Hastings and L. M. Corliss, Physical Review **126**, 556 (1962).

[13] G. Lawes, B. Melot, K. Page, C. Ederer, M. A. Hayward, Th. Proffen, and R. Seshadri, Phys. Rev. B **74**, 024413 (2006)

[14] E. Prince: J. Appl. Phys. **32**, 68S (1961)

[15] R. Tackett, G. Lawes, B. C. Melot, M. Grossman, E. S. Toberer, and R. Seshadri, Phys. Rev. B **76**, 024409 (2007).

[16] R. N. Bhowmik, R. Ranganathan, and R. Nagarajan, Phys. Rev. B **73**, 144413 (2006).

[17] Suzuki, K. Adachi, and T. Katsufuji, J. Phys.: Conf. Ser. **31**, 235 (2006).